ACS Macro Letters

Letter

pubs.acs.org/macroletters

Synthesis of Multicompartment Nanoparticles of Block Copolymer through Two Macro-RAFT Agents Co-Mediated Dispersion Polymerization

Shentong Li, Xin He, Quanlong Li, Pengfei Shi, and Wangqing Zhang*

Key Laboratory of Functional Polymer Materials of the Ministry of Education, Collaborative Innovation Center of Chemical Science and Engineering (Tianjin), Institute of Polymer Chemistry, Nankai University, Tianjin 300071, China

Supporting Information

ABSTRACT: A new and efficient strategy to synthesize multicompartment block copolymer nanoparticles (MCBNs) by two macro-RAFT agents comediated dispersion polymerization is proposed. By simultaneously employing two macro-RAFT agents in dispersion RAFT polymerization, one-pot synthesis of well-defined MCBNs constructed with two diblock copolymers of poly(*tert*-butyl methyl acrylate)-*block*-polystyrene (P*t*BMA-*b*-PS) and poly[*N*-(4-vinylbenzyl)-*N*,*N*-diethylamine]-*block*-polystyrene (PVEA-*b*-PS) is achieved. These MCBNs contain a PS core and discrete PVEA and/or P*t*BMA nodules on the PS core. By changing the ratio of the two macro-RAFT agents or the polymerization degree of the solvophobic block in the two diblock copolymer mixture, the structure of MCBNs can be tuned. Our strategy overcomes the inconvenience and difficulty in synthesis of MCBNs, and it introduces a valid way to prepare well-defined MCBNs constructed with two or more diblock copolymers.

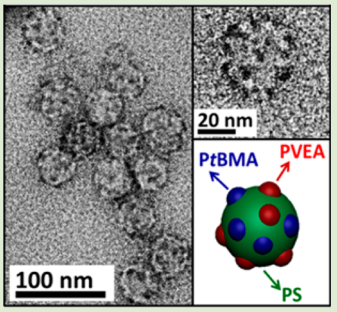

Multicompartment block copolymer nanoparticles (MCBNs) consisting of a solvophilic corona and a solvophobic microphase-segregated core, whose concept draws inspiration from blood proteins such as serum albumin, have aroused great interest for their diverse applications.[1] The microphase-segregated core in MCBNs allows transporting multi-incompatible payloads simultaneously as similar as serum albumin.[1] Generally, there are two strategies to synthesize MCBNs: (1) micellization of linear ABC or BAC triblock terpolymers,[2−15] ABC miktoarm star terpolymers,[16−21] and ABCA or ABCBA multiblock copolymers,[22] in which A represents the solvophilic block and B and C represent the incompatible solvophobic blocks. Through proper choice of the architecture and composition of the copolymers and the processing conditions, a wide diversity of MCBNs have been prepared.[3−22] This micellization strategy suffers from the inconvenience in the synthesis of the complex polymers such as fluorinated terpolymers or miktoarm star terpolymers; and (2) comicellization or blending of two different block copolymers.[23−36] The structure of the MCBNs constructed with two or more block copolymers can be tuned by changing the ratio of the block copolymers in the blended polymers. However, besides the targeted MCBNs constructed with two block copolymers, this comicellization or blending strategy unavoidably leads to nonergodic micelles constructed with one block copolymer.[37] Moreover, since the exchange dynamics between nonergodic micelles is generally very slow,[31−34,38,39] converting nonergodic micelles into mixed micelles or MCBNs by intermicelle macromolecular exchange is very difficult. Up to now, synthesis of well-defined MCBNs suffers from great inconvenience.

Recently, the synthetic method based on polymerization-induced self-assembly (PISA) has been used to prepare well-defined and concentrated AB diblock copolymer nano-objects under dispersion condition.[40] Following this method, a soluble macromolecular RAFT agent (macro-RAFT agent) acting as A block, the monomer to form the insoluble B block and initiator are one-pot added, and RAFT polymerization under dispersion condition is performed. In the initial RAFT polymerization, the growing AB diblock copolymer is molecularly soluble in the polymerization medium since the B block is short. With the proceeding of the RAFT polymerization, the solvophobic B block extends, which drives the self-assembly of the AB diblock copolymer at a critic polymerization degree (DP) of the B block and ultimately the in situ synthesis of AB diblock copolymer nano-objects.[41] Up to now, various block copolymer nano-objects including nanospheres, nanorods, and vesicles with polymer concentration up to 30% have been prepared through the PISA strategy.[42−45]

In this contribution, a new and efficient strategy to synthesize MCBNs constructed with two diblock copolymers, as shown in Scheme 1, is proposed. The strategy includes (1) the two macro-RAFT agents comediated dispersion polymerization of styrene in the ethanol/water mixture (95/5 by weight) to prepare the mixed corona−core nanoparticles of poly(*tert*-butyl methyl acrylate)-*block*-polystyrene (P*t*BMA-*b*-PS) and poly[*N*-(4-vinylbenzyl)-*N*,*N*-diethylamine]-*block*-polystyrene (PVEA-*b*-PS) and (2) deposition of the corona-forming P*t*BMA and

Received: July 29, 2014
Accepted: August 29, 2014
Published: September 3, 2014

Scheme 1. Schematic Synthesis of MCBNs through the Two Macro-RAFT Agents Co-Mediated Dispersion Polymerization

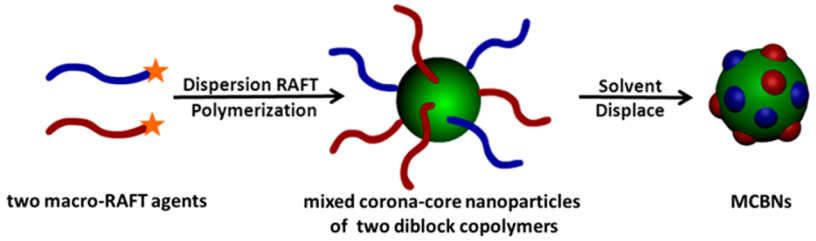

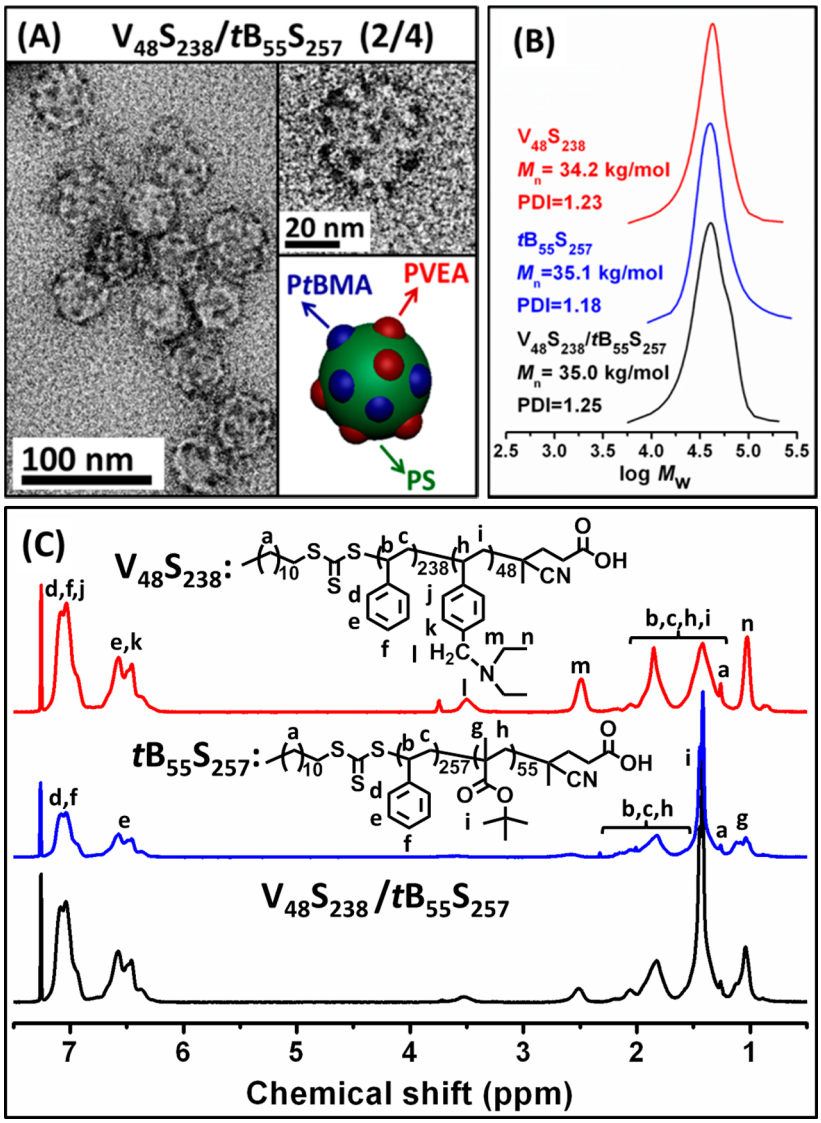

Figure 1. TEM images and the schematic structure of MCBNs of $V_{48}S_{238}/tB_{55}S_{257}$ (2:4; A), the GPC traces (B), and ^{1}H NMR spectra (C) of the $V_{48}S_{238}/tB_{55}S_{257}$ mixture and the separated diblock copolymers of $V_{48}S_{238}$ and $tB_{55}S_{257}$.

PVEA block onto the PS core to form MCBNs containing a PS core and discrete PVEA and P*t*BMA nodules. For briefness, V, *t*B, and S represent the PVEA, P*t*BMA, and PS blocks, and the two diblock copolymers are labeled as VS and *t*BS in the subsequent discussion. This strategy to prepare MCBNs has three advantages. First, it affords one-pot synthesis of MCBNs with polymer concentration up to 20 wt %. Second, it avoids formation of nonergodic micelles constructed with individual block copolymer, since simultaneous comicellization of the in situ synthesized VS/*t*BS mixture occurs during the dispersion RAFT polymerization at low monomer conversion or at low DP of the PS block. Third, the structure of MCBNs can be easily tuned by changing the ratio of the two macro-RAFT agents and the DP of the PS block during the two macro-RAFT agents comediated dispersion polymerization.

The two macro-RAFT agents, poly(*tert*-butyl methyl acrylate) trithiocarbonate ($PtBMA_{55}$-TTC, the molecular weight by GPC analysis $M_{n,GPC}$ = 8.3 kg/mol, PDI = 1.08) and poly[*N*-(4-vinylbenzyl)-*N*,*N*-diethylamine] trithiocarbonate ($PVEA_{48}$-TTC, $M_{n,GPC}$ = 9.4 kg/mol, PDI = 1.22), were

dx.doi.org/10.1021/mz500466x | *ACS Macro Lett.* 2014, 3, 916−921

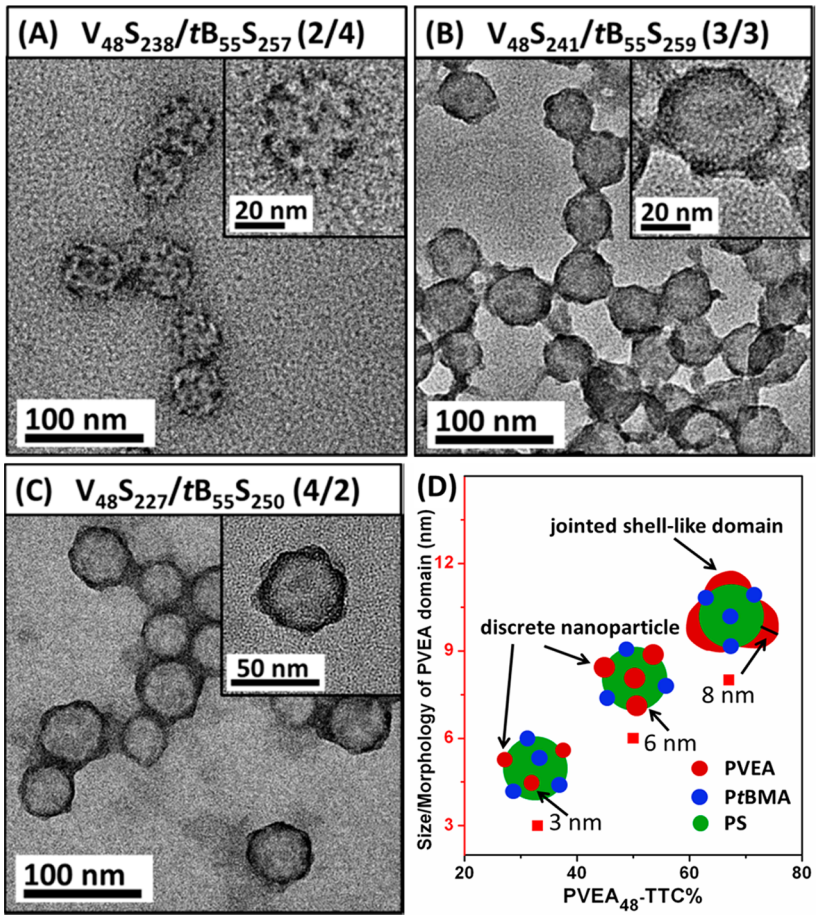

Figure 2. TEM images of MCBNs prepared with the molar ratio of the $PVEA_{48}$-TTC/P*t*BMA_{55}-TTC macro-RAFT agents at 2:4 (A), 3:3 (B), and 4:2 (C), and a summary of the $PVEA_{48}$-TTC percent affecting the morphology of MCBNs (D).

synthesized by RAFT polymerization (seeing the characterization in Figure S1), and two special attentions were taken in the RAFT synthesis. First, P*t*BMA_{55}-TTC and $PVEA_{48}$-TTC have similar DP, since the DP of the macro-RAFT agent can exert great influence on the polymerization kinetics under PISA condition.[44] As shown in Figure S2, the two cases of the individual macro-RAFT agent mediated dispersion polymerization under $[monomer]_0/[macro\text{-}RAFT]_0/[initiator]_0$ = 900:3:1 have very similar polymerization kinetics, and onset of micellization of VS and *t*BS takes place at the same time of 12 h. Thus, in the two macro-RAFT agents co-mediated dispersion polymerization, co-micellization of VS and *t*BS occurs, and the mixed corona−core nanoparticles containing a P*t*BMA/PVEA mixed corona and a PS core, as shown in Scheme 1, are formed. Second, either P*t*BMA or PVEA shows different solubility in the ethanol/water mixture with different water content.[46] For example, P*t*BMA_{55}-TTC and $PVEA_{48}$-TTC are soluble in the polymerization medium of the 95/5 ethanol/water mixture and in pure ethanol, whereas both of them become insoluble in water. Thus, deposition of the corona-forming P*t*BMA and PVEA block onto the PS core of the mixed corona−core nanoparticles can be easily achieved by changing the solvent character or by solvent displacement.

The two macro-RAFT agents comediated dispersion polymerization under $[styrene]_0/[PVEA_{48}\text{-}TTC]_0/[P\textit{t}BMA_{55}\text{-}TTC]_0/[initiator]_0$ = 900:1:2:1 ran similarly with the individual macro-RAFT agent mediated dispersion polymerization, in which an initial 12 h homogeneous polymerization and a subsequent heterogeneous one were observed. After 24 h polymerization, the polymerization was quenched at 80.1% monomer conversion, and the colloidal dispersion of the VS/*t*BS mixed corona−core nanoparticles with polymer concentration at 21.5 wt % was prepared. The colloidal dispersion was dialyzed against ethanol to remove the residual monomer of styrene, then dispersed in water, and last the morphology was checked by TEM. From the TEM image shown in Figure 1A, MCBNs containing a PS core with average diameter D_c at 40 nm and the PVEA nodules with average size D_n at 3 nm are clearly discerned. Note: the MCBN nanoparticles were stained initially with phosphotungstic acid and then with RuO_4; therefore, the gray region is ascribed to the PS core, the discrete dark domain is due to the PVEA nodules, and the P*t*BMA phase is invisible, as discussed elsewhere.[9−11] It is expected that the P*t*BMA block also forms discrete nodules on the PS core, since P*t*BMA is immiscible with PS or PVEA, as discussed previously.[46,47] By checking the two reference nano-objects constructed with one diblock copolymer, the 34 nm P*t*BMA_{55}-*b*-PS_{263} nanoparticles (Figure S3A) and the 170 nm $PVEA_{48}$-*b*-PS_{238} vesicles (Figure S3B), the great difference in the morphology of the synthezied MCBNs, the P*t*BMA_{55}-*b*-PS_{263} nanoparticles and the $PVEA_{48}$-*b*-PS_{238} vesicles is clearly found, confirming the MCBNs being constructed with two diblock copolymers. Note: the 34 nm P*t*BMA_{55}-*b*-PS_{263} nanoparticles and the 170 nm $PVEA_{48}$-*b*-PS_{238} vesicles were prepared through the individual macro-RAFT agent mediated dispersion polymerization under $[styrene]_0/[macro\text{-}RAFT]_0/$

dx.doi.org/10.1021/mz500466x | *ACS Macro Lett.* 2014, 3, 916−921

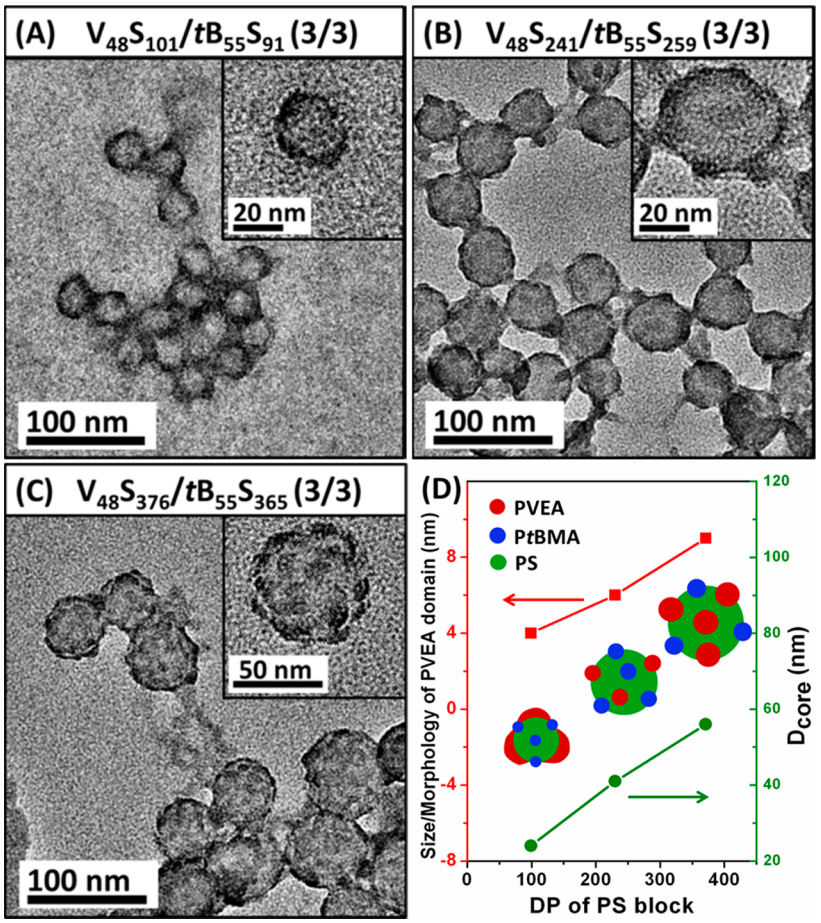

Figure 3. TEM images of MCBNs prepared with the theoretical DP of the PS block in the VS/*t*BS diblock copolymers at 99 (A), 230 (B), and 370 (C), and a summary of the DP of the PS block affecting the morphology of MCBNs (D).

$[\text{initiator}]_0$ = 900:3:1 at 79.4 and 78.2% monomer conversion in 24 h, and the two diblock copolymers have very similar composition with those in MCBNs shown in Figure 1. The formation of discrete PVEA nodules but not an uninterrupted shell on the PS core is due to the PVEA chains being segregated by the neighboring P*t*BMA chains during the PVEA chains depositing on the PS core in the solvent displace.

To detect the composition of MCBNs, separation of the individual diblock copolymer from the VS/*t*BS mixture was performed (see the separation detail in Supporting Information), and the polymers before and after separation were characterized by GPC analysis (Figure 1B) and ^{1}H NMR analysis (Figure 1C). By checking the proton resonance signals at δ = 6.15−7.21 ppm and 3.47 ppm, it is concluded that successful separation is achieved. Based on the ^{1}H NMR spectra and GPC traces of the VS/*t*BS mixture before and after separation, the molar ratio of VS/*t*BS in MCBNs, the molecular weight $M_{n,GPC}$, and PDI of the individual diblock copolymers are obtained, and the results are summarized in Table S1. Therefore, the MCBNs shown in Figure 1 are labeled as $V_{48}S_{238}/tB_{55}S_{257}$ (2:4), in which the DP of the PS block is determined by $M_{n,GPC}$ and the ratio in the bracket represents the molar ratio of VS/*t*BS in MCBNs. It is found that, the NMR-determined molar ratio of $V_{48}S_{238}/tB_{55}S_{257}$ in MCBNs is very close to that of the feeding macro-RAFT agents of PVEA$_{48}$-TTC/P*t*BMA$_{55}$-TTC (2:4.16 vs 2:4), suggesting that almost all of the two macro-RAFT agents are block-extended to form the corresponding diblock copolymers. Besides, it is found that the two diblock copolymers, $V_{48}S_{238}$ and $tB_{55}S_{257}$, have very similar molecular weight and low PDI, as indicated by the insets in Figure 1B, and the reason is due to the similar polymerization kinetics in the dispersion RAFT polymerization.

It is found that the PVEA nodules on MCBNs can be tuned by changing the molar ratio of the PVEA$_{48}$-TTC/P*t*BMA$_{55}$-TTC macro-RAFT agents. As shown in Figure 2, all the MCBNs prepared through the two macro-RAFT agents co-mediated dispersion polymerization under $[\text{styrene}]_0/[\text{two macro-RAFT agents}]_0/[\text{initiator}]_0$ = 900:3:1 contain a PS core with similar D_c at 40−44 nm. This similar D_c of the three MCBNs is due to the very similar DP of the PS block in the VS/*t*BS diblock copolymers, as pointed out at the top of the TEM images in Figure 2. Whereas, the size or morphology of the PVEA domains on the PS core of MCBNs is firmly dependent on the percent of the PVEA$_{48}$-TTC macro-RAFT agent in the PVEA$_{48}$-TTC/P*t*BMA$_{55}$-TTC mixture or the molar ratio of PVEA$_{48}$-TTC/P*t*BMA$_{55}$-TTC (Note: the molar ratio of PVEA$_{48}$-TTC/P*t*BMA$_{55}$-TTC is very close or equal to the molar ratio of VS/*t*BS in MCBNs as discussed above). With the increasing percent of the PVEA$_{48}$-TTC macro-RAFT agent, the PVEA morphology changes from the discrete 3 nm nodules (Figure 2A) to 6 nm nodules (Figure 2B) and, last, to the jointed shell-like microdomain with the maximum thickness at 8 nm (Figure 2C), which is schematically summarized in Figure 2D. This morphology evolution of the PVEA microdomain with the increasing percent of the PVEA$_{48}$-TTC macro-RAFT agent can be explained by the increasing amount of the PVEA

dx.doi.org/10.1021/mz500466x | *ACS Macro Lett.* 2014, 3, 916−921

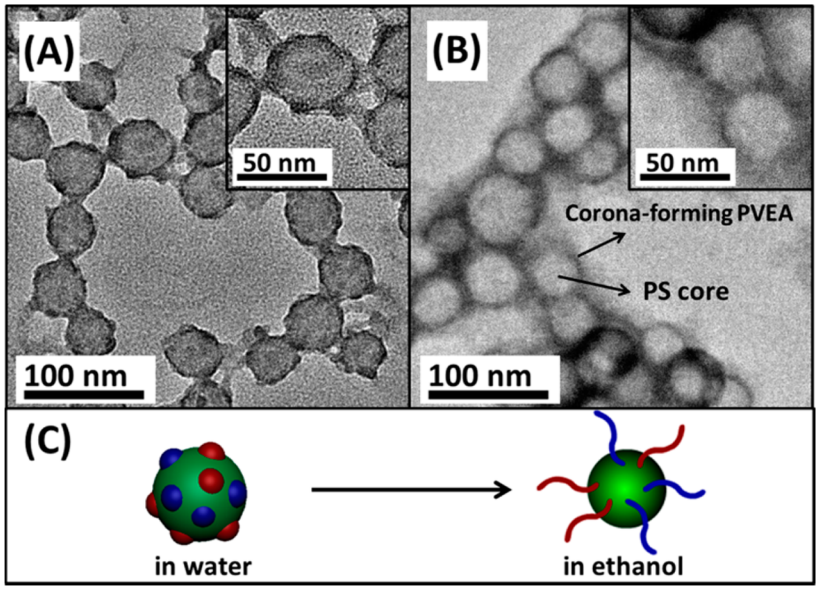

Figure 4. TEM images of the MCBNs of $V_{48}S_{241}/tB_{55}S_{259}$ dispersed in water (A) and the mixed corona−core nanoparticles dispersed in ethanol (B), and the schematic transition of MCBNs to mixed corona−core nanoparticles (C).

chains on the PS core of MCBNs. In the case of a low amount of the PVEA chains, the PVEA chains deposit on the PS core to form discrete PVEA nodules; with the increasing amount of the PVEA chains, the PVEA nodules become larger or are linked together to form jointed shell-like microdomains.

It is also found that the MCBNs structure can be tuned by changing the DP of the PS block (DP_S) in the VS/*t*BS diblock copolymers. Through the two macro-RAFT agents comediated dispersion polymerization under $[styrene]_0/[PVEA_{48}\text{-}TTC]_0/[PVEA_{48}\text{-}TTC]_0/[initiator]_0$ = 450:1.5:1.5:1, 900:1.5:1.5:1 and 1500:1.5:1.5:1 at 65.8−76.5% monomer conversion, MCBNs as shown in Figure 3A−C with the theoretical DP_S at 99, 230, and 370 were prepared (Note: the theoretical DP_S was calculated according to ref 48) by assuming the same DP_S in the VS and *t*BS diblock copolymers, and it was found that the theoretical DP_S was very close to that determined by GPC analysis, as indicated in Figure 3). By statistical analysis of above 100 MCBNs, the structure evolution of MCBNs with DP_S is summarized in Figure 3D. It is found that the diameter of the PS core, D_c, increases from 24 to 56 nm when the theoretical DP_S increases from 99 to 370. The increasing D_c of MCBNs with the theoretical DP_S is due to the PS block extension during the dispersion RAFT polymerization, which is just similarly with those of nanoparticles constructed with one block copolymer prepared through the individual macro-RAFT agent mediated dispersion polymerization.[42−44] Besides, with DP_S increasing, the PVEA morphology on the PS core changes from the jointed shell-like microdomain with the maximum thickness at 4 nm (Figure 3A) to the 6 nm nodules (Figure 3B) and further to the discrete 9 nm nodules (Figure 3C), which is somewhat reverse to the evolution shown in Figure 2. This morphology evolution of the PVEA block on the PS core can be explained by the decreasing specific surface area of the PS core with the extension of the PS block. At the case of the small-sized PS core, more PVEA chains are tethered on per area unit of the PS core than those at the case of large-sized PS core, and therefore, the PVEA chains tend to form the jointed shell-like microdomain at the former case and the discrete nodules at the latter one.

The present synthesis of MCBNs is compared with the blending strategy. After blending the presynthesized 34 nm $PtBMA_{55}$-*b*-PS_{263} nanoparticles (Figure S3A) and the 170 nm $PVEA_{48}$-*b*-PS_{238} vesicles (Figure S3B) in the 95/5 ethanol/water mixture or in ethanol for a given time (Note: ethanol is a better solvent than the 95/5 ethanol/water mixture for the two diblock copolymers), the block copolymer morphology was checked. As shown in Figures S4 and S5, nanoparticles and vesicles but not MCBNs were observed even after 7 days of blending, suggesting no obvious intermicelle macromolecular exchange between the $PtBMA_{55}$-*b*-PS_{263} nanoparticles and the $PVEA_{48}$-*b*-PS_{238} vesicles. This slow or negligible intermicelle macromolecular exchange is due to the high polymer molecular weight, which makes the polymer chains frozen in solvent as discussed elsewhere.[31−34,36,37,49]

Lastly, it is found that MCBNs of VS/*t*BS can reversely convert into mixed corona−shell nanoparticles. When the typical MCBNs of $V_{48}S_{241}/tB_{55}S_{259}$ dispersed in water (Figure 4A) were transferred into ethanol, which is solvent for the $PVAE_{48}$ block and the $PtBMA_{55}$ block, the microdomains of PVEA and P*t*BMA on the PS core are dissolved, and therefore mixed corona−shell nanoparticles (Figure 4B) containing a PS core and a PVAE/P*t*BMA mixed corona are formed (Note: the corona-forming PVEA is indicated by the shadow and the corona-forming P*t*BMA is invisible). The transition of MCBNs to mixed corona−core nanoparticles by selectively dissolving the PVEA/P*t*BMA microdomains is schematically shown in Figure 4C.

Summarily, a new and efficient strategy of synthesis of well-defined multicompartment nanoparticles (MCBNs) constructed with two diblock copolymers through the two macro-RAFT agents comediated dispersion polymerization is proposed. Our strategy has the advantages of the one-pot synthesis of concentrated MCBNs and the tunable structure of MCBNs by changing the molar ratio of the two macro-RAFT agents or the DP of the solvophobic block in the diblock copolymers. Our strategy of the two macro-RAFT agents comediated dispersion polymerization broads an efficient way

dx.doi.org/10.1021/mz500466x | *ACS Macro Lett.* 2014, 3, 916−921

to prepare well-defined MCBNs constructed with two or more than two diblock copolymers, which is ongoing in our lab.

■ ASSOCIATED CONTENT

Supporting Information

The experimental sections and supplementary figures and tables. This material is available free of charge via the Internet at http://pubs.acs.org.

■ AUTHOR INFORMATION

Corresponding Author

*E-mail: wqzhang@nankai.edu.cn.

Notes

The authors declare no competing financial interest.

■ ACKNOWLEDGMENTS

The financial support by National Science Foundation of China (No. 21274066) and PCSIRT (IRT1257) is gratefully acknowledged.

■ REFERENCES

(1) Moughton, A. O.; Hillmyer, M. A.; Lodge, T. P. *Macromolecules* **2012**, *45*, 2−19.
(2) Jiang, T.; Wang, L.; Lin, S.; Lin, J.; Li, Y. *Langmuir* **2011**, *27*, 6440−6448.
(3) Kubowicz, S.; Baussard, J.-F.; Lutz, J.-F.; Thünemann, A.-F.; von Berlepsch, H.; Laschewsky, A. *Angew. Chem., Int. Ed.* **2005**, *44*, 5262−5265.
(4) Marsat, J.-N.; Heydenreich, M.; Kleinpeter, E.; von Berlepsch, H.; Böttcher, C.; Laschewsky, A. *Macromolecules* **2011**, *44*, 2092−2105.
(5) Cui, H.; Chen, Z.; Zhong, S.; Wooley, K. L.; Pochan, D. J. *Science* **2007**, *317*, 647−650.
(6) Sun, G.; Cui, H.; Lin, L. Y.; Lee, N. S.; Yang, C.; Neumann, W. L.; Freskos, J. N.; Shieh, J. J.; Dorshow, R. B.; Wooley, K. L. *J. Am. Chem. Soc.* **2011**, *133*, 8534−8543.
(7) Gröschel, A. H.; Walther, A.; Löbling, T. I.; Schacher, F. H.; Schmalz, H.; Müller, A. H. E. *Nature* **2013**, *503*, 247−251.
(8) Fang, B.; Walther, A.; Wolf, A.; Xu, Y.; Yuan, J.; Müller, A. H. E. *Angew. Chem., Int. Ed.* **2009**, *48*, 2877−2880.
(9) Schacher, F.; Walther, A.; Ruppel, M.; Drechsler, M.; Müller, A. H. E. *Macromolecules* **2009**, *42*, 3540−3548.
(10) Gröschel, A. H.; Walther, A.; Löbling, T. I.; Schmelz, J.; Hanisch, A.; Schmalz, H.; Müller, A. H. E. *J. Am. Chem. Soc.* **2012**, *134*, 13850−13860.
(11) Gröschel, A. H.; Schacher, F. H.; Schmalz, H.; Borisov, O. V.; Zhulina, E. B.; Walther, A.; Müller, A. H. E. *Nat. Commun.* **2012**, *3*, 1−10.
(12) Uchman, M.; Štěpánek, M.; Procházka, K.; Mountrichas, G.; Pispas, S.; Voets, I. K.; Walther, A. *Macromolecules* **2009**, *42*, 5605−5613.
(13) Kyerematen, S. O.; Busse, K.; Kohlbrecher, J.; Kressler, J. *Macromolecules* **2011**, *44*, 583−593.
(14) Gao, Y.; Li, X.; Hong, L.; Liu, G. *Macromolecules* **2012**, *45*, 1321−1330.
(15) Huo, F.; Li, S.; Li, Q.; Qu, Y.; Zhang, W. *Macromolecules* **2014**, *47*, 2340−2349.
(16) Li, Z.; Kesselman, E.; Talmon, Y.; Hillmyer, M. A.; Lodge, T. P. *Science* **2004**, *306*, 98−101.
(17) Li, Z.; Hillmyer, M. A.; Lodge, T. P. *Langmuir* **2006**, *22*, 9409−9417.
(18) Liu, C.; Hillmyer, M. A.; Lodge, T. P. *Langmuir* **2008**, *24*, 12001−12009.
(19) Saito, N.; Liu, C.; Lodge, T. P.; Hillmyer, M. A. *Macromolecules* **2008**, *41*, 8815−8822.
(20) Saito, N.; Liu, C.; Lodge, T. P.; Hillmyer, M. A. *ACS Nano* **2008**, *4*, 1907−1912.
(21) Hanisch, A.; Gröschel, A. H.; Förtsch, M.; Drechsler, M.; Jinnai, H.; Ruhland, T. M.; Schacher, F. H.; Müller, A. H. E. *ACS Nano* **2013**, *7*, 4030−4041.
(22) Gohy, J.-F.; Ott, C.; Hoeppener, S.; Schubert, U. S. *Chem. Commun.* **2009**, 6038−6040.
(23) Srinivas, G.; Pitera, J. W. *Nano Lett.* **2008**, *8*, 611−618.
(24) Zheng, R.; Liu, G.; Yan, X. *J. Am. Chem. Soc.* **2005**, *127*, 15358−15359.
(25) Yan, X.; Liu, G.; Hu, J.; Willson, C. G. *Macromolecules* **2006**, *39*, 1906−1912.
(26) Zhu, J.; Hayward, R. C. *Macromolecules* **2008**, *41*, 7794−7797.
(27) Price, E. W.; Guo, Y.; Wang, C.-W.; Moffitt, M. G. *Langmuir* **2009**, *25*, 6398−6406.
(28) Schacher, F.; Betthausen, E.; Walther, A.; Schmalz, H.; Pergushov, D. V.; Müller, A. H. E. *ACS Nano* **2009**, *3*, 2095−2102.
(29) Christian, D. A.; Tian, A.; Ellenbroek, W. G.; Levental, I.; Rajagopal, K.; Janmey, P. A.; Liu, A. J.; Baumgart, T.; Discher, D. E. *Nat. Mater.* **2009**, *8*, 843−849.
(30) Gohy, J.-F.; Lefèvre, N.; D'Haese, C.; Hoeppener, S.; Schubert, U. S.; Kostov, G.; Améduri, B. *Polym. Chem.* **2011**, *2*, 328−332.
(31) Li, Z.; Hillmyer, M. A.; Lodge, T. P. *Macromolecules* **2006**, *39*, 765−771.
(32) Pochan, D. J.; Zhu, J.; Zhang, K.; Wooley, K. L.; Miesch, C.; Emerick, T. *Soft Matter* **2011**, *7*, 2500−2506.
(33) Zhu, J.; Zhang, S.; Zhang, K.; Wang, X.; Mays, J. W.; Wooley, K. L.; Pochan, D. J. *Nat. Commun.* **2013**, *4*, 1−7.
(34) Zhu, J.; Zhang, S.; Zhang, F.; Wooley, K. L.; Pochan, D. J. *Adv. Funct. Mater.* **2013**, *23*, 1767−1773.
(35) Cheng, L.; Lin, X.; Wang, F.; Liu, B.; Zhou, J.; Li, J.; Li, W. *Macromolecules* **2013**, *46*, 8644−8648.
(36) Liu, X.; Gao, H.; Huang, F.; Pei, X.; An, Y.; Zhang, Z.; Shi, L. *Polymer* **2013**, *54*, 3633−3640.
(37) Yoo, S. I.; Sohn, B.-H.; Zin, W. C.; Jung, J. C.; Park, C. *Macromolecules* **2007**, *40*, 8323−8328.
(38) Jain, S.; Bates, F. S. *Macromolecules* **2004**, *37*, 1511−1523.
(39) Choi, S.-H.; Lodge, T. P.; Bates, F. S. *Phys. Rev. Lett.* **2010**, *104*, 047802.
(40) Charleux, B.; Delaittre, G.; Rieger, J.; D'Agosto, F. *Macromolecules* **2012**, *45*, 6753−6765.
(41) Sun, J.-T.; Hong, C.-Y.; Pan, C.-Y. *Soft Matter* **2012**, *8*, 7753−7767.
(42) Li, Y.; Armes, S. P. *Angew. Chem., Int. Ed.* **2010**, *49*, 4042−4046.
(43) Sugihara, S.; Blanazs, A.; Armes, S. P.; Ryan, A. J.; Lewis, A. L. *J. Am. Chem. Soc.* **2011**, *133*, 15707−15713.
(44) Dan, M.; Huo, F.; Zhang, X.; Wang, X.; Zhang, W. *J. Polym. Sci., Part A: Polym. Chem.* **2013**, *51*, 1573−1584.
(45) Pei, Y.; Lowe, A. B. *Polym. Chem.* **2014**, *5*, 2342−2351.
(46) Li, S.; Huo, F.; Li, Q.; Gao, C.; Su, Y.; Zhang, W. *Polym. Chem.* **2014**, *5*, 3910−3918.
(47) Qin, S.-H.; Qiu, K.-Y. *J. Polym. Sci., Part A: Polym. Chem.* **2001**, *39*, 1450−1455.
(48) Brouwer, H. D.; Schellekens, M. A. J.; Klumperman, B.; Monteiro, M. J.; German, A. L. *J. Polym. Sci., Part A: Polym. Chem.* **2000**, *38*, 3596−3603.
(49) Nicolai, T.; Colombani, O.; Chassenieux, C. *Soft Matter* **2010**, *6*, 3111−3118.